Available online at www.sciencedirect.com
SCIENCE DIRECT
Tectonophysics 416 (2006) 229–244
TECTONOPHYSICS
www.elsevier.com/locate/tecto

Attenuation, transport and diffusion of scalar waves in textured random media

L. Margerin *

Laboratoire de Géophysique Interne et Tectonophysique, Université Joseph Fourier/CNRS, BP 53, 38041, Grenoble, France

Accepted 28 November 2005
Available online 13 February 2006

Abstract

Most theoretical investigations of seismic wave scattering rely on the assumption that the underlying medium is statistically isotropic. However, deep seismic soundings of the crust as well as geological observations often reveal the existence of elongated or preferentially oriented scattering structures. In this paper, we develop mean field and radiative transfer theories to describe the attenuation and multiple scattering of a scalar wavefield in an anisotropic random medium. The scattering mean free path is found to depend strongly on the propagation direction. We derive a radiative transfer equation for statistically anisotropic random media from the Bethe–Salpeter formalism and propose a Monte Carlo method to solve this equation numerically. At longer times, the energy density is shown to obey a tensorial diffusion equation. The components of the diffusion tensor are obtained in closed form and excellent agreement is found between Monte Carlo simulations and analytical solutions of the diffusion equation. The theory has important potential implications for lithospheric models where scatterers are for example flat structures preferentially aligned along the surface. In this simple geometry, analytical expressions of the Coda Q parameter can be given explicitly in the diffusive regime. Our results suggest that pulse broadening and coda decay are controlled by different parameters, related to the eigenvalues of the diffusion tensor. These eigenvalues can differ by more than one order of magnitude. This theory could be applied to probe the anisotropy of length scales in the lithosphere.

Keywords: Multiple scattering; Radiative transfer; Random media; Anisotropy; Coda

1. Introduction

The propagation of seismic waves in heterogeneous media is a topic of continued interest for seismologists. Among the many approaches of the subject, stochastic theories have undergone a vigorous development in the last 20 years. The traditional range of application includes the modeling of the amplitude and phase of coherent arrivals, as well as the transport of the scattered energy. Important advances in the understanding of direct seismic wave attenuation due to scattering have been made by Sato (1982), Wu (1982), Shapiro and Kneib (1993), who developed new theories with specific application to seismic experiments. As an example, the travel-time corrected mean wave formalism of Sato (1982) has nicely reconciled known discrepancies between seismic measurements of attenuation and standard mean field theories. The study of seismic wave travel times in random media has also led to unexpected results. It has for example been shown that the first arrivals can propagate at velocities that are

* Tel.: +33 4 76 82 80 25; fax: +33 4 76 82 81 01.
E-mail address: Ludovic.Margerin@ujf-grenoble.fr.

0040-1951/$ - see front matter © 2005 Elsevier B.V. All rights reserved.
doi:10.1016/j.tecto.2005.11.011

significantly higher than the volume-averaged velocity. This phenomenon has been termed 'velocity shift' and numerous extensive studies can be found in the literature (see, e.g. Roth et al., 1993; Shapiro et al., 1996).

Beyond a length scale known as the mean free path a large part of the energy of the coherent waves has been transferred to scattered waves which eventually form the coda of short period seismic events. The scattered waves transport the energy at distances larger than the mean free path and are responsible for the rapid field fluctuations, which are averaged out in the mean field approach. Thus, the information pertaining to the energy transport in a scattering medium is contained in the second statistical moment of the field. Field–field correlation theory is an extremely powerful tool that establishes the link between wave and radiative transfer equations and provides a theoretical background to explain many striking wave phenomena, such as electron's localization in condensed matter (Vollhardt and Wölfle, 1982), or coherent backscattering of optical waves (Akkermans et al., 1988). Correlation theory of random fields has also known some remarkable achievements in seismology with the development of coda wave interferometry (Snieder et al., 2002) or the Green function reconstruction from coda waves (Campillo and Paul, 2003). These methods make use of the phase information contained in multiply scattered waves to gain information about the medium. Such approaches go beyond the scope of this paper where attention will mostly be given to the energy density.

In seismology, the acoustic transport equation has been introduced by Wu (1985). Later, the theory has been extended to time-dependent cases by Zeng et al. (1991), Sato (1995), and to elastic waves including mode conversions by Zeng (1993) and Sato (1994). Data analysis tools such as the multiple-lapse-time-window analysis have been developed and applied in numerous regions of the world (e.g. Fehler et al., 1992; Hoshiba et al., 2001). Recent years have seen the emergence of even more realistic and challenging modelings including the possible depth dependence of background velocities and scattering properties (Margerin et al., 1998; Hoshiba et al., 2001; Lacombe et al., 2003), the interpretation of short period scattered waves at the global scale (Margerin and Nolet, 2003; Shearer and Earle, 2004) and the scattering of long period Rayleigh waves (Sato and Nishino, 2002). In most of these works, radiative transfer is introduced as a phenomenological theory, leaving a gap with the underlying wave equation. However, in condensed matter physics, radiative transfer emerges as a rigorous consequence of correlation theory, and this is the approach that will be adopted throughout the paper.

Although anisotropic media play a fundamental role in explaining many seismic observations such as anomalous splitting of core-sensitive normal modes or shear wave birefringence, most studies on multiple scattering of seismic waves assume implicitly that the underlying medium is statistically isotropic (see however the works of Iooss, 1998; Samuelides and Mukerji, 1998; Müller and Shapiro, 2003; Kravtsov et al., 2003). Yet, deep seismic soundings and geological maps often reveal elongated or laminated structures (see, e.g. Thybo, 2002). Thus, a scattering theory of anisotropic random media would be a useful tool to quantify the potential impact of textured geological structures on the wavefield. Important efforts have been invested in the study of wave propagation through anisotropic random media, mostly in optics and condensed matter physics. Furutsu (1980) proposed a phenomenological acoustic radiative transfer equation with broken rotational symmetry, and developed a diffusion approximation based on a diagonalization of the collision operator by perturbation theory. Anisotropic random media have also been studied by Wölfle and Bhatt (1984), in connection with the problem of electron localization. A stationary electromagnetic transport equation has been derived by Mischenko (2002) for arbitrarily shaped discrete scatterers using the Lax–Tversky's theory. A radiative transfer theory has also been proposed for electromagnetic waves propagating through nematic liquid crystals (van Tiggelen et al., 1996; Stark and Lubensky, 1997), and some experiments have been conducted (Wiersma et al., 2000; Johnson et al., 2002) that reveal an anisotropic transport of light.

The primary goal of the present work will be to investigate through a simple model, where mode conversions are neglected, how preferentially oriented and shaped inhomogeneities influence the transport of energy. We will employ the Dyson and Bethe–Salpeter formalism developed in condensed matter physics to quantify the attenuation of the mean field and derive from first principles a radiative transfer equation for scalar waves in anisotropic random media. We shall use the term 'anisomeric' random media since this refers to an isotropy of scale lengths. At longer times, the diffuse intensity will be shown to obey a tensorial diffusion equation that can be solved analytically. We will present numerical solutions of the anisotropic transfer equation and comparisons with diffusion theory. Finally, we will apply the diffusion theory to an anisomeric waveguide (for example the earth's crust) to show that broadening of seismogram envelopes and Coda Q may be used to

infer the anisotropy of scale lengths in the medium. An analytical expression of Coda Q including the leakage effect (Margerin et al., 1998, 1999; Wegler, 2004) will also be derived.

2. Presentation of the model

2.1. Examples of anisotropic random media

Anisotropy is a phenomenon that has several possible origins. Crystals such as olivine possess the most fundamental form of anisotropy, which is related to the spatial arrangements of atoms. Yet, a piece of rock which is made of randomly oriented olivine grains will behave as an isotropic elastic body. Hence, anisotropy requires a preferential alignment of the grains in the whole sample. But anisotropy can also be caused by the presence of laminated isotropic structures as is well-known in the theory of 1-D randomly layered media (e.g. Shapiro and Hubral, 1998). The anisotropy that we consider in this paper is of statistical nature and is often referred to as anisomery (Rytov et al., 1989). We imagine that the medium contains scatterers that look like lentils or cigars that are preferentially aligned. At the microscopic scale, described by the wave equation, the medium is perfectly isotropic. But at the macroscopic scale, that is beyond the mean free path, the random medium will display anisotropic attenuation and transport properties.

2.2. Quantitative description of statistical anisotropy

We consider scalar waves propagating in a medium where the velocity fluctuates around a mean value c_0. In a given realization of the statistical ensemble of random media, the field u at frequency ω satisfies the following Helmoltz equation:

$$\Delta u + k_0^2(1+\epsilon(\mathbf{r}))u = 0, \tag{1}$$

where possible source terms have been omitted. The field describes fluctuations in inverse slowness squared. In most cases, one assumes that the power spectrum Φ of the fluctuations is a function of the norm of the wavenumber $\mathbf{k}$ only, which is equivalent to saying that the field is isotropic. For example, the power spectrum of Gaussian random media can be expressed as:

$$\Phi(k) = (2\pi)^{3/2} a^3 \langle \epsilon^2 \rangle e^{-k^2 a^2/2}, \tag{2}$$

where $\langle \epsilon^2 \rangle$ is the total variance of the squared slowness fluctuations and a is the correlation length. This spectrum can be seen as a special case of the more general expression:

$$\Phi(\mathbf{k}) = (2\pi)^{3/2} abc \langle \epsilon^2 \rangle e^{-\frac{1}{2}(k_x^2 a^2 + k_y^2 b^2 + k_z^2 c^2)}, \tag{3}$$

where different correlation lengths have been introduced along the axis $(\hat{\mathbf{x}}, \hat{\mathbf{y}}, \hat{\mathbf{z}})$ of a Cartesian coordinate system. Eq. (3) can be rewritten as:

$$\Phi(\mathbf{k}) = (2\pi)^{3/2} a^3 \langle \epsilon^2 \rangle e^{-k^2 l(\hat{\mathbf{k}})^2/2}, \tag{4}$$

where l can be understood as a correlation length that depends on the space direction $\hat{\mathbf{k}}$. The hat symbol will be used throughout the paper to denote a unitary vector. Depending on the choice of a, b, c, the scatterers take different forms. Let us clarify this on a simple example where we introduce cylindrical symmetry by letting $a=b$. Although it is by no means a restriction of the theory, in numerical applications, this cylindrical symmetry will be adopted in the rest of the paper. When $c \gg a$, the inhomogeneities look like elongated cigars, while in the opposite case they look like squashed-flat objects. This interpretation is valid in a statistical sense only and it has to be emphasized that media with very different spatial distributions of heterogeneity can have exactly the same correlation function. The procedure that has been adopted above can be applied to other correlation functions. As is well-known the power spectrum of isotropic exponential media reads:

$$\Phi(k) = \frac{8\pi abc \langle \epsilon^2 \rangle}{(1+k^2 a^2)^2}, \tag{5}$$

and can be generalized to the anisotropic case as follows:

$$\Phi(\mathbf{k}) = \frac{8\pi abc \langle \epsilon^2 \rangle}{(1+k_x^2 a^2 + k_y^2 b^2 + k_z^2 c^2)^2}. \tag{6}$$

For the moment, we have only considered the spectral representation of inhomogeneities. Yet, another customary method of description is the correlation function, i.e., the inverse Fourier transform of the power spectrum. For Gaussian media, the result is trivial because of the well-known properties of the Fourier transform. As regards the power spectrum (6), the correlation function can be expressed as:

$$C(\mathbf{r}) = \frac{ac \langle \epsilon^2 \rangle e^{-r/\sqrt{a^2 \sin^2\theta + c^2 \cos^2\theta}}}{\sqrt{(a^2\cos^2\theta + c^2 \sin^2\theta)(a^2 \sin^2\theta + c^2 \cos^2\theta)}}, \tag{7}$$

where the additional symmetry $a=b$ has been introduced for simplicity, and θ denotes the angle between the position vector, $\mathbf{r}$, and the axis of symmetry of the system, $\hat{\mathbf{z}}$. Formula (7) shows that the correlation in real space is exponential with a correlation length that depends on the space direction. This agrees with the terminology "exponential power spectrum" used above, and justifies the intuitive procedure used to introduce statistical anisotropy. For a more general introduction to correlation functions in seismology, we refer to Klimeš (2002).

3. Mean free path and phase velocity

We now introduce the multiple scattering formalism in order to determine the phase velocity and spatial decay rate of a coherent plane wave propagating in direction $\hat{\mathbf{p}}$, in an anisomeric random medium. This coherent wave is defined as the ensemble average response of the medium. Like in an isotropic medium, one expects both an attenuation of the coherent wave due to scattering, and a slight shift of the propagation velocity. At a given frequency ω the coherent field excited by a point source G – the mean Green function – obeys the following Dyson equation in wavenumber space (Economou, 1990):

$$G(\omega,\mathbf{p})=\frac{(2\pi)^3}{k_0^2-p^2-(2\pi)^{-3}\Sigma(\omega,\mathbf{p})}, \tag{8}$$

where k_0 is the wavenumber in the reference medium, and Σ is a new object known as the self-energy or mass operator. Σ can be considered as a unit-cell from which all the possible scattering paths in the random medium can be constructed. Eq. (8) is exact but cannot be solved unless an approximate form of Σ is introduced. To lowest order of the perturbations $\langle\epsilon^2\rangle$, the mass operator is given by (Frisch, 1968):

$$\Sigma(\omega,\mathbf{p})=\frac{k_0^4}{(2\pi)^3}\int_{\mathbb{R}^3}G_0(\omega,\mathbf{q})\Phi(\mathbf{p}-\mathbf{q})d^3q. \tag{9}$$

Eq. (9) is known as the Bourret or first-order smoothing approximation. Physically, it implies that the waves can visit an arbitrary number of inhomogeneities, provided they are different. Thus, recurrent scattering is not taken into account, which is accurate for sufficiently small perturbations. In Eq. (9), G_0 denotes the Green function of the reference medium:

$$G_0(\omega,\mathbf{p})=\frac{(2\pi)^3}{k_0^2-p^2+i\eta}, \tag{10}$$

where η is a positive and infinitesimal imaginary part which ensures that the retarded solution is selected. As usual, the location of the poles of the mean Green function provides the dispersion relation in the random medium (Sheng, 1995). This is still a complicated task because the poles are solutions of an integral equation. It is customary to further simplify the problem by assuming that the wavenumber inside any inhomogeneity differs very little from k_0, which is also known as Born approximation (Weaver, 1990). One then obtains the following explicit expression of the effective wavenumber k_e in the random medium:

$$k_e(\omega,\hat{\mathbf{p}})=k_0-\frac{1}{2(2\pi)^3k_0}\Re\{\Sigma(\omega,k_0\hat{\mathbf{p}})\}-i\frac{1}{2(2\pi)^3k_0}\Im\{\Sigma(\omega,k_0\hat{\mathbf{p}})\}, \tag{11}$$

where symbols $\Re$, $\Im$ denote the real and imaginary part, respectively. The product of the inverse real part of the effective wavenumber with the frequency defines the phase velocity v. Eq. (11) also shows that any plane wave propagating in the random medium has a finite imaginary part. As is well-known, this has nothing to do with absorption but reflects the amplitude decay of the coherent wave caused by the random scattering events. In scattering theory, $1/(2\Im\{k_e\})$ is defined as the mean free path l, which is the length scale beyond which a significant amount of energy has been scattered away from the incident direction. At this point it is useful to introduce the following functional limit ($\eta\to0^+$):

$$G_0(\omega,\mathbf{p})=(2\pi)^3\left[\mathrm{P.V.}\frac{1}{k_0^2-p^2}-i\pi\delta(k_0^2-p^2)\right], \tag{12}$$

which enables to derive simple expressions for v and l:

$$\frac{\omega}{v(\hat{\mathbf{p}})}=k_0+\frac{k_0^3}{16\pi^3}\mathrm{P.V.}\int_{\mathbb{R}^3}\frac{1}{q^2-k_0^2}\Phi(k_0\hat{\mathbf{p}}-\mathbf{q})d^3q, \tag{13}$$

$$\frac{1}{l(\hat{\mathbf{p}})}=\frac{k_0^4}{16\pi^2}\int_{4\pi}\Phi(k_0\hat{\mathbf{p}}-k_0\hat{\mathbf{q}})d^2\hat{\mathbf{q}}. \tag{14}$$

In Eqs. (12) and (13), the symbol P.V. denotes the Cauchy principal value, and the formula assumes that the parameter $\langle\epsilon^2\rangle$ of the power spectrum Φ represents the total variance of the squared-slowness (which is 4 times larger than the variance of velocity). These results put forward the angular dependence of both v and l. The Cauchy principal value can be evaluated numerically by regularizing the integrand, a procedure which is frequently encountered in the literature in connection with Kramers–Krönig relations (see, e.g. Byron and Fuller, 1992, p. 346). The angular integration in Eq. (14)

poses no special problem. Eqs. (13) and (14) are very general and will now be applied to Gaussian and exponential media possessing a rotational symmetry axis ($a=b$ in Eqs. (6) and (3)), as depicted in Fig. 1. In this geometry, l and v only depend on the polar angle θ between the wavevector and the axis of symmetry. This case is very relevant to seismological applications and is relatively easier to investigate.

In Fig. 2, we illustrate the angular dependence of the mean free path and phase velocity in an exponential medium with 5% rms velocity fluctuations, fixed correlation length $a=0.5$ and varying correlation length $c=1, 2, 3, 4, 5$. The wavenumber in the reference medium is normalized to one. With increasing c, the scatterers tend to look more and more like elongated cigars. Broader range of parameters have been investigated but it was found that the effects of anisomery become important only in the regime $\max(k_0a, k_0c) \geq 1/2$, that is when the wavelength and the size of the objects become comparable. The upper bound of the correlation lengths is imposed by the condition of validity of the Bourret approximation $\max(k_0^2a^2\langle\epsilon^2\rangle, k_0^2c^2\langle\epsilon^2\rangle) \ll 1$ (Rytov et al., 1989). Physically this means that a wave propagating through a scatterer acquires a negligible phase delay. In Fig. 2, it is noticeable that the difference between the phase velocity in the reference medium and in the random medium never exceeds 0.5%. Thus, the slowness surface can hardly be distinguished from a spherical surface with radius $1/\overline{v} = 1/4\pi \int_{4\pi} 1/v(\hat{\mathbf{p}}) d^2\hat{\mathrm{p}}$. In certain directions the phase velocity can exceed the reference value c_0, which is never the case in an isotropic medium (Rytov et al., 1989). This does not constitute a violation of causality because our approximation automatically verifies the Kramers–Krönig relations. It is also to be noted that the phase velocity averaged over all propagation directions is always smaller than c_0. These

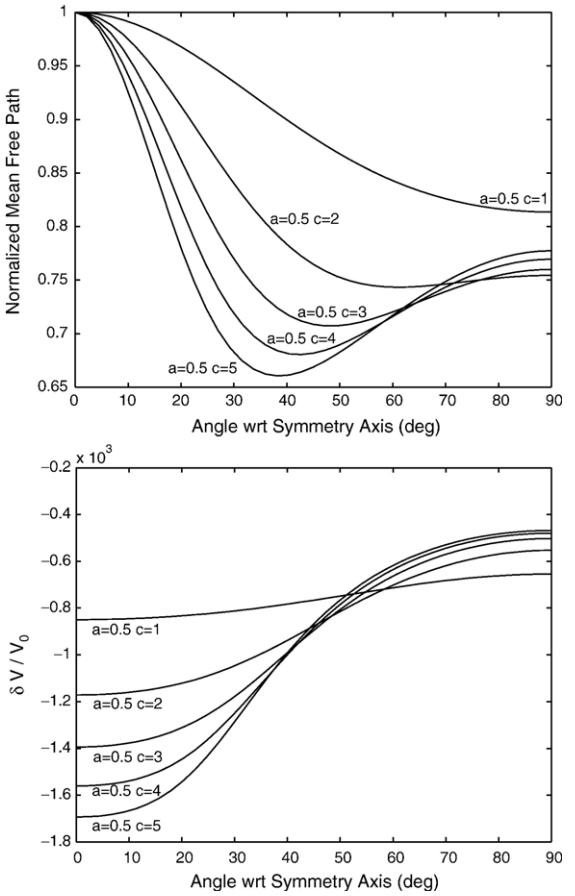

Fig. 2. Top: angular dependence of the mean free path in an exponential anisotropic medium with $a=0.5$ and $c=1, 2, 3, 4, 5$ and rms velocity fluctuations 5%. For each curve, the maximum of the mean free path has been normalized to 1. Bottom: angular dependence of the *perturbation* of phase velocity (same medium). The correlation lengths are indicated next to each curve. The angle θ between the wavevector and the symmetry axis varies between 0° and 90° only because the medium is invariant by reflection with respect to a plane perpendicular to this axis.

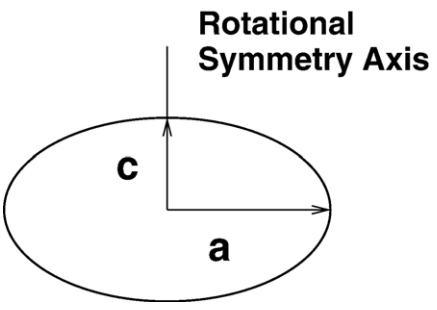

Fig. 1. Schematic view of the geometry of the random medium. The random medium is assumed to have rotational symmetry with respect to a fixed axis. The correlation length equals c along the symmetry axis, and a along any perpendicular direction.

features are further illustrated in Fig. 3, which is similar to Fig. 2 but with $a=4.5$ and $c=1, 2, 3, 4, 5$. With decreasing c, the scatterers tend to look more and more squashed flat. In Fig. 4, we also show the results of calculations with $a=2.5$ and $c=1, 2, 3, 4, 5$. Our calculations imply that the anisotropy of scale lengths cannot explain the strong velocity anisotropy sometimes observed in the Earth. Even by boosting the perturbations up to 10%, the deviation from isotropy would still be less than 1%, but the theory may break down for such large perturbations. Finally, we comment on the limits of validity of the theory for the case of extremely flat scatterers ($c \to 0$, $a \to \infty$, see Fig. 1). In that case, the medium can be considered as

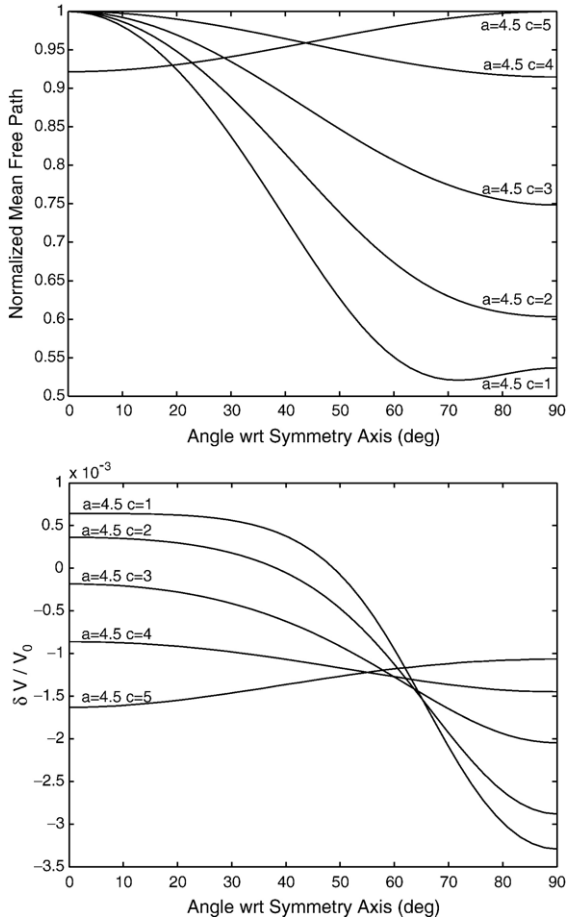

Fig. 3. Top: angular dependence of the mean free path in an exponential anisotropic medium with $a=5.0$ and $c=1, 2, 3, 4, 5$ and rms velocity fluctuations 5%. For each curve, the maximum of the mean free path has been normalized to 1. Bottom: angular dependence of the *perturbation* of phase velocity (same medium). The correlation lengths are indicated next to each curve. The angle θ between the wavevector and the symmetry axis varies between 0° and 90° only because the medium is invariant by reflection with respect to a plane perpendicular to this axis.

locally layered. For such finely layered media, transport theory is known to break down because of interference effects between multiply reflected/transmitted waves, and localization theory should then be applied (Shapiro and Hubral, 1998).

It is noticeable that the scattering mean free path depends very strongly on the propagation direction. This dependence is rich and complex and it is apparent that the extrema of the mean free path do not necessarily coincide with the principal axes of the medium. In a random medium composed of very flat objects with anisotropy parameter $c/a=9$, (see Fig. 1) the ratio between the max and min mean free path can be as large as 2, which would certainly be detectable if the mean field could accurately be measured. Note that in most cases, seismologists do not have access to the mean field but rather to its travel-time corrected version. In this case, the measured attenuation length can differ significantly from the mean free path as has been explained by Sato (1982) and Wu (1982). These authors also developed theoretical approaches such as the travel-time corrected mean wave formalism, which are in better agreement with the seismological practice. We do not discuss these theories in this paper, but it is anticipated that the attenuation length should still depend strongly on the propagation direction.

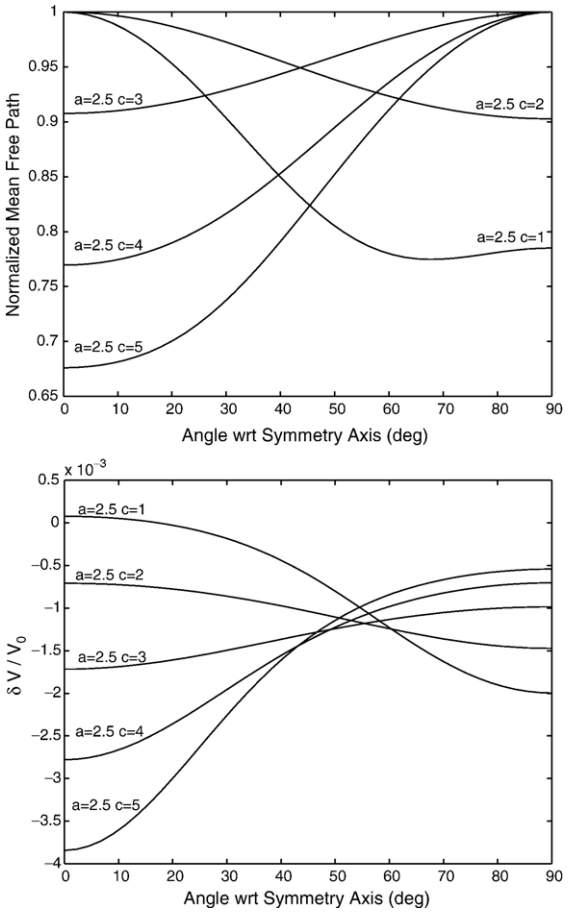

Fig. 4. Top: angular dependence of the mean free path in an exponential anisotropic medium with $a=2.5$ and $c=1, 2, 3, 4, 5$ and rms velocity fluctuations 5%. For each curve, the maximum of the mean free path has been normalized to 1. Bottom: angular dependence of the *perturbation* of phase velocity (same medium). The correlation lengths are indicated next to each curve. The angle θ between the wavevector and the symmetry axis varies between 0° and 90° only because the medium is invariant by reflection with respect to a plane perpendicular to this axis.

4. Transport theory

4.1. General definitions and approximations

Beyond one mean free path, most of the energy has been transferred from the coherent wave to diffuse scattered waves which will form the coda of the seismic signal. As will be shown below, the space–time distribution of energy in the coda is governed by a radiative transfer equation. We present a concise derivation of this equation for an anisomeric random medium. We first introduce the energy density of the scalar field u for a source at $\mathbf{r}'$ and detection at $\mathbf{r}$ as:

$$E(t,\mathbf{r},\mathbf{r}') \approx \frac{1}{2}\left| c_0^{-1}\frac{\partial}{\partial t}u(t,\mathbf{r},\mathbf{r}')\right|^2 + E_{\mathrm{p}}, \tag{15}$$

where c_0 is the velocity in the reference medium and E_{p} denotes the potential energy. Note that Eq. (15) assumes that the velocity departs only slightly from c_0. Following Weaver (1990), we assume that the virial theorem applies and focus our attention on the first term, i.e. the kinetic energy. The field can be decomposed over different frequency components by Fourier transformation:

$$u(t,\mathbf{r},\mathbf{r}') = \frac{1}{2\pi}\int_{\mathbb{R}} u(\omega,\mathbf{r},\mathbf{r}')e^{-i\omega t}d\omega. \tag{16}$$

which yields the following expression for the intensity:

$$E(t)=\frac{1}{(2\pi)^2}\iint_{\mathbb{R}^2}\omega_1\omega_2 u(\omega_1)u^{\star}(\omega_2)e^{-i\omega_1 t+i\omega_2 t}\mathrm{d}\omega_1\mathrm{d}\omega_2, \tag{17}$$

where the star denotes complex conjugate and constant prefactors have been dropped. For notational simplicity, the dependence on the spatial variables $\mathbf{r}$ and $\mathbf{r}'$ is omitted. Upon introducing the barycentric variables $\omega=(\omega_1+\omega_2)/2$ and $\omega_d=\omega_1-\omega_2$, the intensity can in turn be written as a Fourier integral:

$$E(\Omega)=\frac{1}{(2\pi)^2}\iiint_{\mathbb{R}^3}(\omega+\omega_d/2)(\omega-\omega_d/2) \times u(\omega+\omega_d/2)u^{\star}(\omega-\omega_d/2)e^{-i\omega_d t+i\Omega t}\mathrm{d}\omega\mathrm{d}\omega_d\mathrm{d}t. \tag{18}$$

Integration over time yields a $2\pi\delta(\Omega-\omega_d)$ factor and further integration over ω_d gives:

$$E(\Omega) = \frac{1}{(2\pi)}\int_{\mathbb{R}}(\omega+\Omega/2)(\omega-\Omega/2) \times u(\omega+\Omega/2)u^{\star}(\omega-\Omega/2)\mathrm{d}\omega. \tag{19}$$

We now assume that the field u is narrowly band-passed which means that $E(\Omega)$ will be non-zero for $\Omega \ll \omega$ only. Because Ω is the conjugate variable of the time t, this implies that the intensity evolution is slow compared to the typical oscillation period of the field. This separation of time scales is known as the slowly varying envelope approximation. In agreement with signal theory terminology, ω and Ω are sometimes referred to as the carrier (or internal) frequency, and the modulation (or external) frequency, respectively. Following Weaver (1990), we invoke an ergodic hypothesis and assume that integrating over the internal frequency is equivalent to an ensemble average. Taking into account the band-passed nature of u, one finds the following approximate expression:

$$E(\Omega,\mathbf{r},\mathbf{r}')\approx\frac{\omega^2\Delta\omega}{2\pi c_0^2}\langle u(\omega+\Omega/2,\mathbf{r},\mathbf{r}')u^{\star}(\omega-\Omega/2,\mathbf{r},\mathbf{r}')\rangle, \tag{20}$$

where $\Delta\omega$ is the typical bandwidth of the signal, and brackets denote an ensemble average. From the preceding argument, it becomes clear that the density of radiation per unit frequency $\mathcal{E}=2\pi E/\Delta\omega$ can be obtained from the two-point, two-frequency correlation function defined as:

$$\langle u(\omega+\Omega/2,\mathbf{R}+\mathbf{r}/2)u^{\star}(\omega-\Omega/2,\mathbf{R}-\mathbf{r}/2)\rangle = \frac{1}{(2\pi)^6}\int\!\!\int_{\mathbb{R}^3}\Gamma_{\omega,\mathbf{p}}(\Omega,\boldsymbol{\Delta})e^{i(\mathbf{p}\cdot\mathbf{r}+\boldsymbol{\Delta}\cdot\mathbf{R})}d^3p d^3\Delta, \tag{21}$$

where $\mathbf{r}$ denotes the separation between the two measurement points, and $\mathbf{R}$ is the position with respect to a point-like source. Since ensemble averaging restores the translational symmetry, the field–field correlation function does not depend explicitly on the source position, which explains the simplified notations (dependence on source position has been dropped). In Eq. (21), Γ is recognized as the spatial Fourier transform of the two-point correlation function of the wavefield. As for temporal variables, we will assume that the average energy distribution is smooth at the wavelength scale. It implies that the energy is carried in space by wavepackets that have fast internal oscillations modulated by a smooth envelope. By identifying p and Δ as the central and modulation wavenumbers of the wavepackets, respectively, we require that $p \ll \Delta$ (Sheng, 1995). In the definition of Γ, the internal variables appear as subscripts, a convention that will be adopted where possible in the following discussion.

4.2. Radiative transfer approximation of the Bethe–Salpeter equation

The correlation theory of random wavefields shows that the two-point correlation function of the wavefield obeys a Bethe–Salpeter equation. This equation has been derived in details in several papers and textbooks and we refer the interested reader to Frisch (1968), Rytov et al. (1989) or van Rossum and Nieuwenhuizen (1999). The Bethe–Salpeter is an exact (perturbative) equation that retains all the possible correlations among the various scattering paths in the medium. In the Fourier domain, this equation writes (Lagendijk and van Tiggelen, 1996):

$$\left[-\frac{\partial k_0^2}{\partial \omega}\Omega + 2\mathbf{p}\cdot\boldsymbol{\Delta} + \frac{\Delta\Sigma_{\omega,\mathbf{p}}(\Omega,\boldsymbol{\Delta})}{(2\pi)^3}\right]\Gamma_{\omega,\mathbf{p}}(\Omega,\boldsymbol{\Delta}) = (2\pi)^3\Delta G_{\omega,\mathbf{p}}(\Omega,\boldsymbol{\Delta}) \times\left[\frac{S(\omega)}{(2\pi)^6}+\frac{1}{(2\pi)^{12}}\int_{\mathbb{R}^3}U_{\omega,\mathbf{p},\mathbf{s}}(\Omega,\boldsymbol{\Delta})\Gamma_{\omega,\mathbf{s}}(\Omega,\boldsymbol{\Delta})d^3s\right], \tag{22}$$

where the following notations have been introduced:

$$\Delta G_{\omega,\mathbf{p}}(\Omega,\boldsymbol{\Delta}) = G\left(\omega+\frac{\Omega}{2},\mathbf{p}+\frac{\boldsymbol{\Delta}}{2}\right)-G^{\star}\left(\omega-\frac{\Omega}{2},\mathbf{p}-\frac{\boldsymbol{\Delta}}{2}\right), \tag{23}$$

with a similar definition for $\Delta\Sigma$; S is a source term that depends on the energy released by the point source in a narrow frequency band around ω. Eq. (22) introduces the new object U known as the Vertex function, which can be interpreted as a unit cell from which all the possible multiple scattering paths involving two fields can be described. For more details about the definition and construction of the Vertex function, the reader is referred to Frisch (1968). As it stands, the Bethe–Salpeter equation is intractable and approximations of U, $\Delta\Sigma$ and ΔG are required. The conservation of energy is an important constraint that must be fulfilled by the approximate expressions. In a stationary situation, a relatively simple equation known as Ward identity, or generalized optical theorem guarantees the conservation of energy (Lagendijk and van Tiggelen, 1996):

$$(2\pi)^6\Delta\Sigma_{\omega,\mathbf{p}}(\Omega,\boldsymbol{\Delta})=\int_{\mathbb{R}^3}\Delta G_{\omega,\mathbf{p}'}(\Omega,\boldsymbol{\Delta})U_{\omega,\mathbf{p}',\mathbf{p}}(\Omega,\boldsymbol{\Delta})d^3p', \tag{24}$$

with $\Omega=0$. When calculating the mean free path, we have already approximated Σ to lowest order of the perturbations. The corresponding approximation of the Vertex function is provided by Frisch (1968):

$$U(\mathbf{p},\mathbf{p}';\mathbf{q},\mathbf{q}') = k_0^4(2\pi)^3\Phi\left(\frac{\mathbf{p}-\mathbf{q}+\mathbf{p}'-\mathbf{q}'}{2}\right). \tag{25}$$

Eq. (25) is often termed the 'ladder' approximation, a term deriving from the diagrammatic representation of U often employed in condensed matter physics. This approximation implies that waves can visit an arbitrary number of inhomogeneities, but neglects the occurrence of recurrent scattering between two (or more) scatterers. It can be shown that the ladder diagrams represent the dominant part of the multiple-scattered wavefield except in a sphere of diameter a wavelength around the source where crossed diagrams representing interference between reciprocal wavepaths contribute an equal amount of energy, giving rise to backscattering enhancement and weak localization (Akkermans et al., 1988; Larose et al., 2004). We now make use of the slowly varying envelope approximation, and note that for sufficiently small Δ, the two terms defining ΔG and $\Delta\Sigma$ nearly become complex conjugates of each other, which yields: $\Delta G \approx -2i\Im\{G\}$, with a similar approximation for Σ. The final step consists in replacing $\Im\{G\}$ by $\Im\{G_0\}\propto -i\pi\delta(k^2-k_0^2)$, which is equivalent to neglecting the renormalization of the phase velocity in the random medium. This is not a severe approximation since we have shown that for rms fluctuations of order 5%, the phase velocity differs by at most 0.5% from the reference value. This is completely equivalent to the Born approximation that has been applied to evaluate the mean free path and phase velocity, where the slight perturbation of velocity inside the scatterer was neglected. Actually, it can be seen that Eq. (25) contains as a special case the definition of the mean free path. The Bethe–Salpeter equation now simplifies to:

$$\left[-ik_0\frac{\partial k_0}{\partial\omega}\Omega + i\mathbf{p}\cdot\boldsymbol{\Delta} - \frac{\Im\{\Sigma(\omega,\mathbf{p})\}}{(2\pi)^3}\right]\Gamma_{\omega,\mathbf{p}}(\Omega,\boldsymbol{\Delta}) = \pi\delta(k_0^2-p^2)\left[S(\omega)+\frac{k_0^4}{(2\pi)^3}\int_{\mathbb{R}^3}\Phi(\mathbf{p}-\mathbf{s})\Gamma_{\omega,\mathbf{s}}(\Omega,\boldsymbol{\Delta})d^3s\right]. \tag{26}$$

The presence of the delta function imposes that Γ be sharply peaked around k_0 and therefore suggests a solution of the form:

$$\Gamma_{\omega,\mathbf{p}}(\Omega,\boldsymbol{\Delta}) = \frac{16\pi^3c_0^2}{\omega^3}\delta(k_0^2-p^2)I_{\omega,\hat{\mathbf{p}}}(\Omega,\Delta), \tag{27}$$

where I denotes the specific intensity (written in the Fourier domain). In Eq. (27), the prefactor has been

chosen in such a way that the specific intensity in the space–time domain, obtained after inverse Fourier transformation over Ω and Δ obeys the customary relation (Chandrasekhar, 1960):

$$\mathcal{E}(t,\mathbf{R}) = \frac{1}{c_0}\int_{4\pi} I_{\omega,\hat{\mathbf{p}}}(t,\mathbf{R}) d^2\hat{\mathbf{p}} \tag{28}$$

where ε denotes the energy density. According to Eq. (21), the specific intensity can be rigorously defined as the angular spectrum of the field correlation function. It can also be understood as an angularly resolved energy flux as illustrated in Eq. (28). This is the usual phenomenological definition encountered in textbooks (e.g. Chandrasekhar, 1960). Noting the following Fourier transform equivalence $\frac{\partial}{\partial t} \leftrightarrow -i\Omega, \nabla_{\mathbf{r}} \leftrightarrow i\Delta$, and using the definition of the mean free path (14), one obtains the radiative transfer equation in anisomeric random media:

$$\frac{\partial I_{\omega,\hat{\mathbf{p}}}(t,\mathbf{R})}{c_0 \partial t} + \hat{\mathbf{p}}\cdot\nabla I_{\omega,\hat{\mathbf{p}}}(t,\mathbf{R}) = -\frac{I_{\omega,\hat{\mathbf{p}}(t,\mathbf{R})}}{l(\hat{\mathbf{p}})} + \int_{4\pi} \sigma(\hat{\mathbf{p}},\hat{\mathbf{p}}') I_{\omega,\hat{\mathbf{p}}'}(t,\mathbf{R}) d^2\hat{\mathbf{p}}' + S_{\omega,\hat{\mathbf{p}}}(t,\mathbf{R}), \tag{29}$$

where the differential scattering cross-section is defined as:

$$\sigma(\hat{\mathbf{p}},\hat{\mathbf{p}}') = \frac{k_0^4}{16\pi^2}\Phi(k_0\hat{\mathbf{p}} - k_0\hat{\mathbf{p}}'), \tag{30}$$

and the energy release by (seismic) sources is encapsulated in S. This equation bears a close resemblance with the transfer equation in an isotropic medium. The term on the left-hand side describes the change of intensity of an energy beam propagating in direction $\hat{\mathbf{p}}$. The first and second terms on the right-hand side represent losses and gains caused by random scattering events, respectively. This equation represents a local detailed energy balance and can be shown to obey energy conservation as it was stated before. In a weak scattering regime and for lapse times t is sufficiently small compared to the man free time $\tau = l/c_0$, the transport equation is equivalent to the usual Born approximation. In addition, the transport equation provides a rigorous description of the energy propagation in the multiple scattering regime $t \geq \tau$. The notable difference between Eq. (29) and the usual transport equation is the explicit dependence of the scattering mean free path on space direction, as well as the explicit dependence of the differential scattering cross-section σ on both the incoming and outgoing propagation directions. σ describes the angular dependence of the scattering pattern and is completely determined by the power spectrum of the fluctuations. It obeys the general reciprocity relation:

$$\sigma(\hat{\mathbf{p}},\hat{\mathbf{p}}') = \sigma(-\hat{\mathbf{p}}', -\hat{\mathbf{p}}). \tag{31}$$

To gain insight into the physics contained in Eq. (29), we will now solve it by two customary methods. First we will investigate asymptotic solutions of the transport equation in the limit ($t \to \infty$). We will find that the energy density obeys a generalized tensorial diffusion equation which can be solved analytically in simple cases. These asymptotic solutions will then be compared to 'exact' numerical solutions of the transport equation by the Monte Carlo method.

5. Diffusive regime

Multiple scattering processes tend to uniformize the angular dependence of intensity because each scattering event distributes energy randomly in phase space. After a sufficiently large number of scattering events, we thus expect the intensity to differ only slightly from isotropy. The physical idea of the diffusion approximation can be expressed mathematically by an expansion of the specific intensity in a linear combination of its first two angular moments. The first moment is simply related to the local energy density:

$$c_0\mathcal{E}(t,\mathbf{R}) = \int_{4\pi} I_{\hat{\mathbf{p}}}(t,\mathbf{R}) d^2\hat{\mathbf{p}}, \tag{32}$$

and the second moment defines the energy current vector $\mathbf{J}$:

$$\mathbf{J}(t,\mathbf{R}) = \int_{4\pi} I_{\hat{\mathbf{p}}}(t,\mathbf{R})\hat{\mathbf{p}} d^2\hat{\mathbf{p}}. \tag{33}$$

The current vector gives the local direction of maximum energy flow. Note that the ω dependence of all quantities has been dropped for notational convenience. Combining Eqs. (32) and (33), the following expansion of the specific intensity is obtained:

$$I_{\hat{\mathbf{p}}}(t,\mathbf{R}) = \frac{c_0}{4\pi}\mathcal{E}(t,\mathbf{R}) + \frac{3}{4\pi}\mathbf{J}(t,\mathbf{R})\cdot\hat{\mathbf{p}} + \cdots, \tag{34}$$

where the dots stand for higher order multipoles that are neglected and the $3/4\pi$ prefactor guarantees the consistency of Eqs. (33) and (34). After integration of the transport equation over the whole solid angle, one obtains the following exact continuity equation:

$$\frac{\partial\mathcal{E}(t,\mathbf{R})}{\partial t} + \nabla\cdot\mathbf{J}(t,\mathbf{R}) = 0, \tag{35}$$

where the source term has been omitted for simplicity. Eq. (35) expresses the conservation of energy in the random medium. The next step is to establish a relation between the spatial gradient of energy density and the current vector. Following the standard procedure, we insert expansion (34) in the transport equation and calculate its second moment. After some algebra, this yields:

$$\mathbf{J}(t,\mathbf{R}) = -\mathbf{D}\nabla\mathcal{E}(t,\mathbf{R}), \tag{36}$$

where $\mathbf{D}$ is a symmetric diffusion tensor. This diffusion tensor can be written in the following suggestive form by analogy with the isotropic case:

$$\mathbf{D} = \frac{c_0\mathbf{L}^\star}{3}, \tag{37}$$

where $\mathbf{L}^\star$ denotes the transport mean free path tensor. In the isotropic case, the transport mean free path tensor is diagonal with elements:

$$l^\star = \frac{l}{1-\langle\hat{\mathbf{p}}\cdot\hat{\mathbf{p}}'\rangle}, \tag{38}$$

where l is the usual (direction independent) scattering mean free path, $\hat{\mathbf{p}}$ and $\hat{\mathbf{p}}'$ are the incoming and outgoing propagation direction. The brackets denote a weighted average over the whole solid angle, where the weighting function is the differential cross-section, which in the isotropic case depends solely on the scalar product $\hat{\mathbf{p}}$ or $\hat{\mathbf{p}}'$. In an anisomeric random medium, the expression of the transport mean free path tensor is far more complex:

$$\mathbf{L}^\star = (\mathbf{K_1}-\mathbf{K_2})^{-1}, \tag{39}$$

where the tensors $\mathbf{K_1}$ and $\mathbf{K_2}$ are fully determined by the power spectrum of heterogeneities:

$$\mathbf{K_1} = \frac{3}{4\pi}\iint_{4\pi}\sigma(\hat{\mathbf{p}},\hat{\mathbf{p}}')\hat{\mathbf{p}}'\otimes\hat{\mathbf{p}}'d^2\hat{p}d^2\hat{p}', \tag{40}$$

$$\mathbf{K_2} = \frac{3}{4\pi}\iint_{4\pi}\sigma(\hat{\mathbf{p}},\hat{\mathbf{p}}')\hat{\mathbf{p}}\otimes\hat{\mathbf{p}}'d^2\hat{p}d^2\hat{p}', \tag{41}$$

where the symbol $\otimes$ denotes the usual tensor product. In the course of the derivation use is made of the reciprocity relation (31), and of the symmetry of the phase function to an inversion: $\hat{\mathbf{p}}\rightarrow-\hat{\mathbf{p}}, \hat{\mathbf{p}}'\rightarrow-\hat{\mathbf{p}}'$. These symmetries should hold for quite a general class of random media and do not represent a restriction of the theory. Contrary to what happens in an isotropic medium, the direction of maximum energy flow does not necessarily coincide with the gradient of the energy density, which is intuitively appealing. Thus the texture of the material tends to "guide" the energy along preferential directions. After inserting relation (36) into the continuity Eq. (35) one obtains the following tensorial diffusion equation for the energy density:

$$\frac{\partial\mathcal{E}(t,\mathbf{R})}{\partial t} - \nabla\cdot\mathbf{D}\nabla\mathcal{E}(t,\mathbf{R}) = S(t,\mathbf{R}), \tag{42}$$

where S denotes a source term. In the next section, we will investigate both numerical and approximate analytical solutions of the transport equation for anisotropic random media.

6. Comparison of Monte Carlo simulations and diffusion approximation

We consider anisotropic random media with a symmetry axis directed along the $\hat{\mathbf{z}}$ (vertical) direction of a Cartesian system (see Fig. 1). By symmetry, the diffusion tensor must be diagonal in the set of axis ($\hat{\mathbf{x}}$, $\hat{\mathbf{y}}$, $\hat{\mathbf{z}}$), where $\hat{\mathbf{x}}$ and $\hat{\mathbf{y}}$ denote orthogonal vectors in the horizontal plane. The eigenvalues of the diffusion tensor *perpendicular* and *parallel* to the $\hat{\mathbf{z}}$ axis will be denoted by $D_{\|}$ and $D_{\perp}$, respectively. The choice for this notation will become clear in the next part of the paper. The analytical solution of the diffusion equation with source term $S(t,\ \mathbf{R})=\delta(t)\delta(\mathbf{R})$ writes (Carslaw and Jaeger, 1959):

$$\mathcal{E}(t,\mathbf{R}) = (4\pi t)^{-3/2}D_{\|}^{-1}D_{\perp}^{-1/2}e^{-[z^2/4D_\perp t+(x^2+y^2)/4D_{\|}t]}. \tag{43}$$

Solving analytically the transport equation is a very difficult task and in most cases, one must resort to numerical methods. Considering the large dimensionality of our problem and the complexity introduced by the anisomery of the medium, Monte Carlo simulations constitute a convenient and flexible tool. This powerful method has already been applied to complex seismological situations and we refer the interested reader to the literature for an introduction to the topic (Hoshiba, 1991; Margerin et al., 1998). The basis of the method can better be understood by using an analogy with the kinetic theory of gases where the radiative transfer equation (known in this field as the Boltzmann equation) is used to model the flow of particles. In this picture, the transport of seismic energy in a scattering medium is analogous to the random walk of many particles that collide and get randomly deflected. The mean free path can therefore be interpreted as the average distance between two collisions. The

normalized differential scattering cross-section σ gives the probability distribution for a transition from state $\hat{\mathbf{p}}$ to state $\hat{\mathbf{p}}'$. From a more technical point of view, two difficulties have to be overcome in the case of an anisomeric random medium. First, we note that the mean free path depends on the propagation direction. This is easily handled by introducing an angular dependent average distance between two collisions. Thus the probability law to determine the free path length L of a particle propagating in direction $\hat{\mathbf{p}}$ is given by $F=-l(\hat{\mathbf{p}})\ \ln(u)$, where u is a uniformly distributed random number in the interval]0, 1[. Second, the differential cross-section depends explicitly on the incoming direction $\hat{\mathbf{p}}'$ and the two angles defining the outgoing direction do not decouple. After normalization, we interpret the differential cross-section as the conditional probability for outgoing state $\hat{\mathbf{p}}$ knowing incoming state $\hat{\mathbf{p}}'$. The outgoing scattering direction is subsequently chosen by applying a rejection algorithm (Press et al., 1992). Note that this technique does not require the introduction of an intermediate local reference frame and provides the new propagation direction directly in the global frame. This advantage is somewhat balanced by the relatively low efficiency of the method when the scattering pattern is highly peaked in certain directions.

We have calculated the point source solutions of the radiative transfer and diffusion equations in Gaussian random media, for both weak and strong scattering media with rms velocity fluctuations equal to 3.5% and 7%, respectively. Two detectors are located 100 km away in the $\hat{\mathbf{x}}$ and $\hat{\mathbf{z}}$ directions, from an isotropic, instantaneous, and point-like source. The central wavenumber of the waves is $k_0=10$ which corresponds to high-frequency (6.4 Hz) waves in a medium with velocity $c_0=4$ km/s. In Fig. 5, we show the results of the calculations for elongated objects ($k_0a=0.6$, $k_0c=2.0$). The diffusion constants have been calculated by means of the theory developed above. We find $D_{\|}=20.4$ km^2/s, $D_{\perp}=66.4$ km^2/s for 7% rms velocity fluctuations, and $D_{\|}=81.6$ km^2/s, $D_{\perp}=265.5$ km^2/s for 3.5% rms, which shows that the transport is more efficient in the direction of elongation of the objects. In the strong scattering medium, the Monte Carlo solutions show irregular and unphysical glitches. These fluctuations of the numerical solution are characteristic of the statistical method and could be damped by increasing the number of realizations. In weak scattering media, the diffusion solution approximates poorly the behavior of the full numerical solution at early times. The Monte Carlo solution confirms that the transport is facilitated along the direction of stretching of the scatterers. At late times,

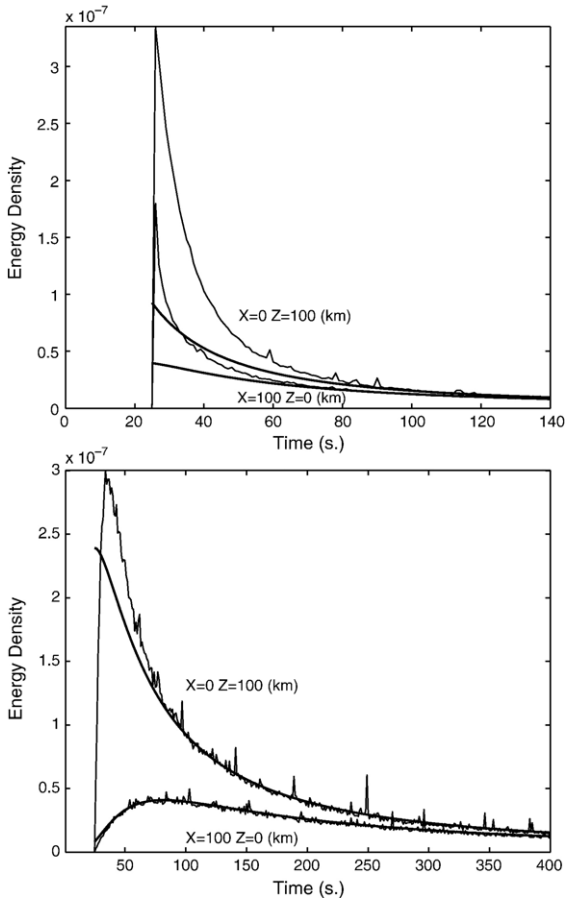

Fig. 5. Energy density as a function time (in seconds) in a Gaussian anisomeric random medium with $k_0a=0.6$ and $k_0c=2$. The point source has unit energy. The location of the receivers is indicated next to each curve. The heavy lines correspond to analytical solutions of the diffusion equation, while the wiggly lines show the results of the Monte Carlo simulations. Top: weak scattering regime (rms velocity fluctuations 3.5%). Bottom: strong scattering regime (rms velocity fluctuations 7%).

both solutions agree very well as expected. The two methods are thus complementary: the diffusion equation yields a simple and accurate approximation at late times, where convergence of the Monte Carlo method is slower and numerical accuracy generally less. In the strong scattering regime it is striking to see how well the diffusion approximation can capture the complex time-dependence of the energy density. The largest difference of order 20% occurs at early times in the direction where the diffusion constant is larger. This is a remarkably good agreement considering the tremendous simplification of the physics introduced in the diffusion approximation. Thus, the diffusion solution can be used as an excellent first guess in solutions of multiple scattering problems. For comparison, we show in Fig. 6

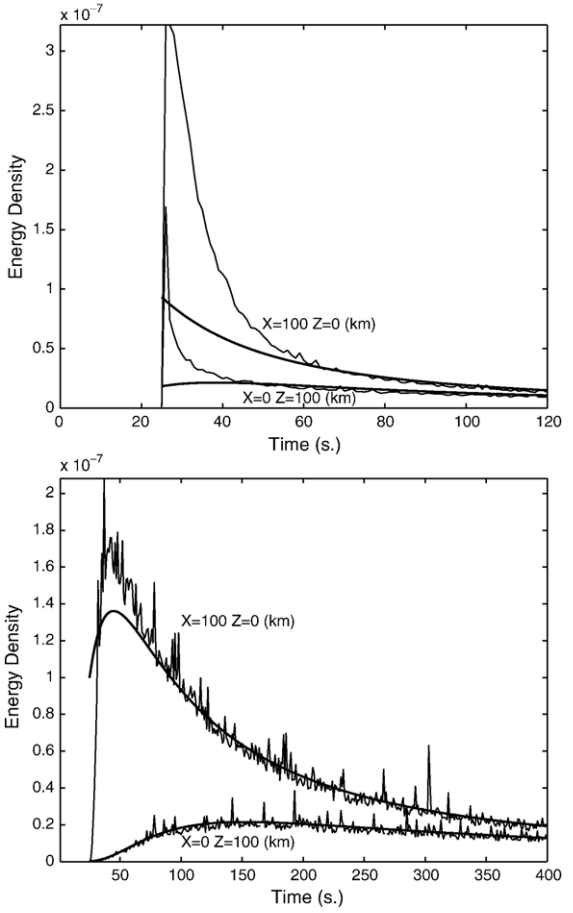

Fig. 6. Energy density as a function time (in seconds) in a Gaussian anisomeric random medium with $k_0a=2.0$ and $k_0c=0.6$. The point source has unit energy. The location of the receivers is indicated next to each curve. The heavy lines correspond to analytical solutions of the diffusion equation, while the wiggly lines show the results of the Monte Carlo simulations. Top: weak scattering regime (rms velocity fluctuations 3.5%). Bottom: strong scattering regime (rms velocity fluctuations 7%).

the results obtained for flat object with $k_0a=2$ and $k_0c=0.6$, with all other parameters unchanged. In this case, one obtains the following diffusion constants: $D_{\|}=37.3$ km^2/s, $D_{\perp}=10.9$ km^2/s with 7% rms, and $D_{\|}=149.1$, $D_{\perp}=43.6$ km^2/s with 3.5% rms. This shows that the energy will be preferentially transported along the direction of flattening of the scatterers. Apart from this difference, the essential features are similar to Fig. 5.

7. Application to a waveguide

For the moment, we have considered the propagation of energy in infinite space. This is not very satisfying since there are major velocity discontinuities inside the earth that cause the reflection of the seismic energy. Below we develop a simple model for the propagation in the lithosphere, as illustrated in Fig. 7. We assume that the lithosphere is composed of a random heterogeneous and anisotropic crust overlying a homogeneous mantle. Such a model has already been shown by Margerin et al. (1999), Hoshiba et al. (2001), Lacombe et al. (2003) to successfully predict the coda decay of regional earthquakes. We further assume that the free surface is perpendicular to the symmetry axis of the anisotropic scatterers as depicted in Fig. 7, i.e. the scatterers are either stretched perpendicular to the surface or flattened parallel to the surface. Taking the $\hat{\mathbf{z}}$ axis perpendicular to the surface, and an arbitrary set $(\hat{\mathbf{x}}, \hat{\mathbf{y}})$ of orthogonal vectors parallel to the surface diagonalizes the diffusion tensor. We call $D_{\|}$ and $D_{\perp}$ the eigenvalues of the diffusion tensor parallel and perpendicular to the free surface, respectively. Our model also includes a step increase of wavespeed at the Moho. We assume that the eigenvalues of the transport mean free path tensor are smaller than the crustal thickness. In this regime, the diffusion approximation should apply (Margerin et al., 1998) but must be supplemented with boundary conditions. They can be obtained by writing down a detailed balance of energy on an infinitesimal portion of interface. The presence of statistical anisotropy does not yield any new difficulties, and we refer the reader to the literature (Zhu et al., 1991; Margerin et al., 1998) for further details of this procedure. Writing down an energy balance at the free surface and at the Moho, one obtains the following boundary conditions, respectively:

$$\frac{\partial \mathcal{E}(t,\mathbf{R})}{\partial z} = 0 \text{ at } z = 0 \tag{44}$$

$$\mathcal{E}(t,\mathbf{R}) + 2c_0^{-1}\gamma D_{\perp}\frac{\partial \mathcal{E}(t,\mathbf{R})}{\partial z} = 0, \text{ at } z = H \tag{45}$$

where γ is a function of the reflection coefficient at the Moho at depth H. The zero flux condition at the surface expresses the total reflection of energy, while the boundary condition at the Moho describes the partial trapping of energy in the crust. The factor γ is related to the usual energy reflection coefficient R at the Moho as follows (Zhu et al., 1991; Margerin et al., 1998):

$$\gamma = \frac{1 + 3\int_0^1 R(\mu)\mu^2 d\mu}{1 - 2\int_0^1 R(\mu)\mu d\mu}, \tag{46}$$

where μ denotes the cosine of the incidence angle. Since the scattering mean free path in the mantle is assumed to

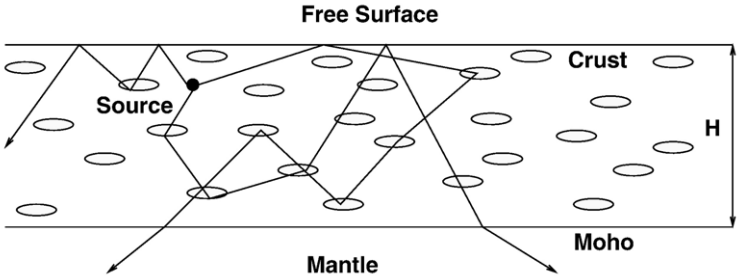

Fig. 7. Schematic view of the wave propagation in a waveguide with statistically anisotropic scatterers, preferentially aligned along the free surface. Note that in a single realization of the random medium, the scatterers are expected to look very different from the cartoon above. H denotes the crustal thickness. As the waves leave the source they are multiply scattered by velocity fluctuations and multiply reflected by the Moho and the free surface. It will be assumed that the mantle is weakly heterogeneous, and does not backscatter a significant amount of energy.

be much larger than in the crust, Eq. (45) neglects the backscattering from the mantle. The system of Eqs. (43−45) can be solved using the results of Margerin et al. (1998), after the following change of variables: $x \to D_\perp x/D_{\|}, y \to D_\perp y/D_{\|}$, which maps the anisotropic diffusion equation onto an isotropic one. For a simple case of a source located near the surface, one obtains:

$$\mathcal{E}(t,\mathbf{R}) \sim t^{-1} e^{(R^2/4D_{\|}t + \omega t/Q_c)}. \tag{47}$$

This expression is formally identical to that proposed by Aki and Chouet (1975) to describe the decay of the coda. The Coda Q parameter Q_c is obtained explicitly as follows:

$$Q_c = \frac{\omega H^2}{D_\perp \xi^2}, \tag{48}$$

where H is the crustal thickness and ξ is the smallest solution of the equation $\xi \tan \xi = H/\gamma$, usually of order 1. Following Margerin et al. (1999), it is also possible to define the residence time of the diffuse waves in the waveguide as:

$$\tau_r = \frac{Q_c}{\omega}. \tag{49}$$

The residence time characterizes the rate of decay of the coda. From Eq. (47), it is possible to derive a characteristic time for the broadening of the seismic pulse τ_b defined as the time to reach the maximum energy density. For sufficiently large source receiver distance R, τ_b can be approximated as:

$$\tau_b \approx \frac{HR}{2\xi\sqrt{D_{\|}D_\perp}}. \tag{50}$$

Formulas (49) and (50) are instructive because they show that in a simple but realistic geometry the broadening of the initial pulse and the coda decay are controlled by independent parameters. $\sqrt{D_{\|}D_\perp}$ governs the lateral spreading of the pulse while $D_\perp$ controls the

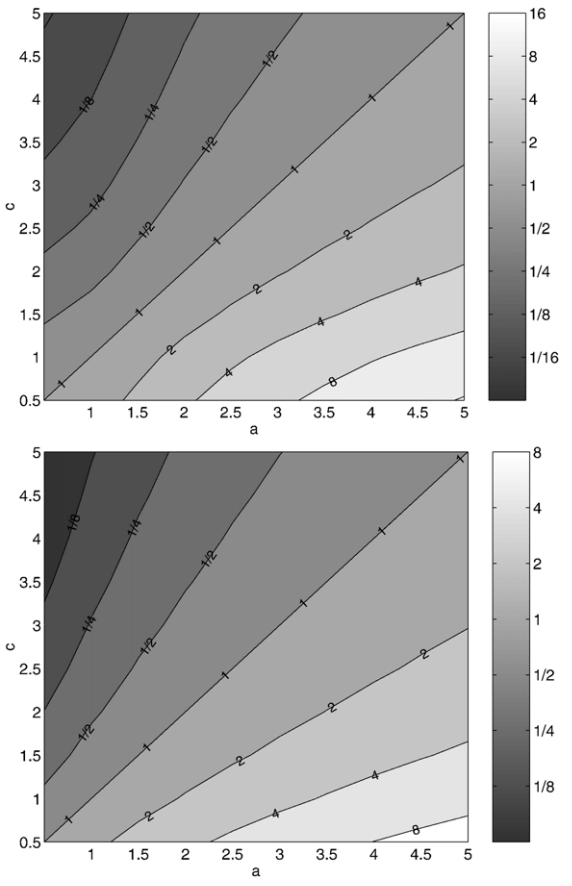

Fig. 8. Contour plot of $\ln(D_{\|}/D_\perp)$ as a function of horizontal (a) and vertical (c) correlation lengths. Labels on the curve indicate the value of the ratio $D_{\|}/D_\perp$. The wavenumber is normalized ($k_0 = 1$). Top: anisotropic Gaussian medium. Bottom: anisotropic exponential medium.

leakage rate of the diffuse waves. In order to evaluate the potential impact of statistical anisotropy on the transport properties, we have studied systematically the ratio of parallel to transverse components of the diffusion tensor in exponential and Gaussian media. The results are shown in Fig. 8 where we plot the natural logarithm of the ratio $D_{\|}/D_{\perp}$ as a function of the vertical and horizontal correlation lengths a and c. Note that we assume that the medium has rotational symmetry around the vertical axis. The results show that the ratio $D_{\|}/D_{\perp}$ can indeed become very large for sufficiently anisotropic media. This in turn implies that values of the transport mean free path inferred from pulse broadening and coda decay can be significantly different.

8. Perspectives and conclusion

In the context of wave propagation in the crust and lithosphere at local and regional distances, the present theory could be applied to infer the anisotropy of scale lengths from the joint analysis of direct and coda wave energy envelops following the work of Abubakirov and Gusev (1990), who measured the scattering properties of the lithosphere under Kamchatka. It is striking that their estimates of the transport mean free path deduced from pulse broadening and coda wave analysis can differ by a factor as large as 2 (see table 1 of Abubakirov and Gusev, 1990). This discrepancy could be reconciled by introducing statistical anisotropy in the earth. Indeed, we have shown that in anisomeric media the broadening of the pulse and the decay rate of the coda are controlled by two different transport mean free paths, in sharp contrast with the isotropic case. The theory of multiple scattering in a waveguide could also be applied to infer the scattering properties of the crust by analyzing the spatio-temporal distribution of energy in the coda of high-frequency (>1 Hz) Lg waves, following the work of Lacombe et al. (2003). Recent modeling of scattering by upper mantle structures (Nielsen et al., 2003) have put forward the role of elongated objects to explain the characteristics of the wavefield at epicentral distances typically smaller than 40 degrees. Transport theory could be used to further investigate the proposed models of scattering by comparing modeled envelopes of multiply-scattered waves with observed short period coda envelopes. At the global scale, transport theory of anisomeric media could be applied to the coda of teleseismic wavefields (Shearer and Earle, 2004) or precursors of some phases such as PKP (Hedlin et al., 1997) and PKKP (Earle and Shearer, 1997). In particular, the energy envelopes of PKP precursors have been extensively studied in recent years (Hedlin and Shearer, 2000; Margerin and Nolet, 2003) in order to determine the depth and size distribution of small-scale heterogeneities in the lower mantle. Cormier (1999) has proposed that anisomeric structures may be superposed onto statistically isotropic fluctuations in the deepest parts of the lower mantle. Our transport equation could be used to model the multiple scattering of P waves in such media and give better constraints on the presence of statistical anisotropy in D''. In conclusion, we have developed a transport theory for acoustic and anisomeric random media, as well as methods of solution. The biggest restriction of the present work is the absence of energy exchange between P and S modes as would be the case for elastic media. Nevertheless, it is hoped that the present results can be used to reveal the signature of anisotropy by analyzing attenuation and transport properties of short period seismic waves.

Acknowledgments

The topic of this paper was motivated by discussions with M. Campillo. I thank my office mate E. Chaljub for numerous advices that greatly helped me in the course of this work. B. van Tiggelen guided me in the multiple scattering formalism and corrected some of my mistakes. Reviewers are acknowledged for suggesting improvements to the original manuscript.

References

Abubakirov, I.R., Gusev, A.A., 1990. Estimation of scattering properties of lithosphere of Kamchatka based on Monte-Carlo simulation of record envelope of a near earthquake. Phys. Earth Planet. Inter. 64, 52–67.

Aki, K., Chouet, B., 1975. Origin of coda waves: source, attenuation, and scattering effects. J. Geophys. Res. 80, 3322–3342.

Akkermans, E., Wolf, P.E., Maynard, R., Maret, G., 1988. Theoretical study of the coherent backscattering of light by disordered media. J. Phys. France 49, 77–98.

Byron, F.W., Fuller, R.W., 1992. Mathematics of Classical and Quantum Physics. Dover, New York.

Campillo, M., Paul, A., 2003. Long range correlations in the diffuse seismic coda. Science 299, 537–540.

Carslaw, H.S., Jaeger, J.C., 1959. Conduction of Heat in Solids, 2 ed. Oxford Sci, Oxford, UK.

Chandrasekhar, S., 1960. Radiative Transfer. Dover, New York.

Cormier, V.F., 1999. Anisotropy of heterogeneity scale lengths in the lower mantle from PKIKP precursors. Geophys. J. Int. 136, 373–384.

Earle, P., Shearer, P., 1997. Observations of PKKP precursors used to estimate small-scale topography on the core-mantle boundary. Science 667–670.

Economou, E.N., 1990. Green's Functions in Quantum Physics. Springer-Verlag, Berlin.

Fehler, M., Hoshiba, M., Sato, H., Obara, K., 1992. Separation of scattering and intrinsic attenuation for the Kanto–Tokai region,

Japan, using measurements of S-wave energy versus hypocentral distance. Geophys. J. Int. 108, 787–800.
Frisch, U., 1968. Wave propagation in random media. In: Bharucha-Reid, A.T. (Ed.), Probabilistic Methods in Applied Mathematics, vol. I. Academic Press, New York, pp. 76–198.
Furutsu, K., 1980. Diffusion equation derived from the space–time transport equation in anisotropic random media. J. Math. Phys. 21, 765–777.
Hedlin, M.A.H., Shearer, P., 2000. An analysis of large-scale variations in small-scale mantle heterogeneity using Global Seismographic Network recordings of precursors to PKP. J. Geophys. Res. 105. doi:10.1029/2000JB900019.
Hedlin, M.A.H., Shearer, P., Earle, P., 1997. Seismic evidence for small-scale heterogeneity throughout the Earth mantle. Nature 387, 145–150.
Hoshiba, M., 1991. Simulation of multiple-scattered coda wave excitation based on the energy conservation law. Phys. Earth Planet. Inter. 67, 123–136.
Hoshiba, M., Rietbrock, A., Scherbaum, F., Nakahara, H., Haberland, C., 2001. Scattering attenuation and intrinsic absorption using uniform and depth dependent model: application to full seismogram envelope recorded in Northern Chile. J. Seismol. 5, 157–179.
Iooss, B., 1998. Seismic reflection traveltimes in two-dimensional statistically anisotropic random medium. Geophys. J. Int. 135, 999–1010.
Johnson, P.M., Bret, B.P.J., Rivas, J.G., Kelly, J.J., Lagendijk, A., 2002. Anisotropic diffusion of light in a strongly scattering material. Phys. Rev. Lett. 89 (art. 243901).
Klimeš, L., 2002. Correlation function of random media. Pure Appl. Geophys. 159, 1811–1831.
Kravtsov, Yu. A., Müller, T.M., Shapiro, S.A., Buske, S., 2003. Statistical properties of reflection traveltimes in 3-D randomly inhomogeneous and anisomeric media. Geophys. J. Int. 154, 841–851.
Lacombe, C., Campillo, M., Paul, A., Margerin, L., 2003. Separation of intrinsic absorption and scattering attenuation from Lg coda decay in central France using acoustic radiative transfer theory. Geophys. J. Int. 154, 417–425.
Lagendijk, A., van Tiggelen, B.A., 1996. Resonant multiple scattering of light. Phys. Rep. 270, 143–215.
Larose, E., Margerin, L., van Tiggelen, B.A., Campillo, M., 2004. Weak localization of seismic waves. Phys. Rev. Lett. 93 (art. 048501).
Margerin, L., Nolet, G., 2003. Multiple scattering of high frequency seismic waves in the deep Earth: PKP precursor analysis and inversion for mantle granularity. J. Geophys. Res. 108 (art. 2514).
Margerin, L., Campillo, M., van Tiggelen, B.A., 1998. Radiative transfer and diffusion of waves in a layered medium: new insight into Coda *Q*. Geophys. J. Int. 134, 596–612.
Margerin, L., Campillo, M., van Tiggelen, B.A., 1999. Residence time of diffuse waves in the crust as a physical interpretation of Coda *Q*: application to seismograms recorded in Mexico. Geophys. J. Int. 138, 343–352.
Mischenko, M.I., 2002. Vector radiative transfer equation for arbitrarily shaped and arbitrarily oriented particles: a microphysical derivation from statistical electromagnetics. Appl. Opt. 41, 7114–7135.
Müller, T.M., Shapiro, S.A., 2003. Amplitude fluctuations due to diffraction and refraction in anisotropic random media: implications for seismic scattering attenuation estimates. Geophys. J. Int. 155, 139–148.
Nielsen, L., Thybo, H., Levander, A., Solodilov, L., 2003. Origin of upper mantle seismic scattering evidence from Russian PNE data. Geophys. J. Int. 154, 196–204.
Press, W.H., Teukolsky, S.A., Vetterling, W.T., Flannery, B.P., 1992. Numerical Recipes in C. The Art of Scientific Computing, Second edition. Cambridge University Press, Cambridge, UK.
Roth, M., Müller, G., Snieder, R., 1993. Velocity shift in random media. Geophys. J. Int. 115, 552–563.
Rytov, S.M., Kravtsov, Yu.A., Tatarskii, V.I., 1989. Principles of Statistical Radiophysics 4; Wave Propagation Through Random Media. Springer-Verlag, Berlin.
Samuelides, Y., Mukerji, T., 1998. Velocity shift in heterogeneous media with anisotropic spatial correlation. Geophys. J. Int. 134, 778–786.
Sato, H., 1982. Amplitude attenuation of impulsive waves in random media based on travel time corrected mean wave formalism. J. Acoust. Soc. Am. 71, 559–564.
Sato, H., 1994. Multiple isotropic scattering model including P–S conversions for the seismogram envelope formation. Geophys. J. Int. 117, 487–494.
Sato, H., 1995. Formulation of the multiple non-isotropic scattering process in 3-D space on the basis of energy transport theory. Geophys. J. Int. 121, 523–531.
Sato, H., Nishino, M., 2002. Multiple isotropic-scattering model on the spherical Earth for the synthesis of Rayleigh-wave envelopes. J. Geophys. Res. 107 (art. 2343).
Shapiro, S.A., Hubral, P., 1998. Elastic Waves in Random Media. Springer, Heidelberg.
Shapiro, S.A., Kneib, G., 1993. Seismic attenuation by scattering: theory and numerical results. Geophys. J. Int. 114, 373–391.
Shapiro, S., Schwarz, R., Gold, N., 1996. The effect of random isotropic inhomogeneities on the phase velocity of seismic waves. Geophys. J. Int. 127, 783–794.
Shearer, P.M., Earle, P.A., 2004. The global short-period wavefield modelled with a Monte-Carlo seismic phonon method. Geophys. J. Int. 158, 1103–1117.
Sheng, P., 1995. Introduction to Wave Scattering, Localization and Mesoscopic Phenomena. Academic Press, San Diego.
Snieder, R., Grêt, A., Douma, H., Scales, J., 2002. Coda wave interferometry for estimating non-linear behavior in seismic velocity. Science 295, 2253–2255.
Stark, H., Lubensky, T.C., 1997. Multiple light scattering in anisotropic random media. Phys. Rev., E 55, 514–533.
Thybo, H. (Ed.), 2002. Deep Seismic Profiling of the Continents. Tectonophysics, vol. 355, pp. 1–263.
van Rossum, M.C.W., Nieuwenhuizen, T.M., 1999. Multiple scattering of classical waves: Microscopy, mesoscopy, and diffusion. Rev. Mod. Phys. 71, 313–371.
van Tiggelen, B.A., Maynard, R., Heiderich, A., 1996. Anisotropic light diffusion in oriented nematic liquid crystals. Phys. Rev. Lett. 77, 639–642.
Vollhardt, D., Wölfle, P., 1982. Scaling equations from a self-consistent theory of Anderson localization. Phys. Rev. Lett. 48, 699–702.
Weaver, R.L., 1990. Diffusivity of ultrasound in polycrystals. J. Mech. Phys. Solids 38, 55–86.
Wegler, U., 2004. Diffusion of seismic waves in a thick layer: theory and application to Vesuvius volcano. J Geophys. Res. 109 art. B07303.
Wiersma, D.S., Muzzi, A., Colocci, M., Righini, R., 2000. Time-resolved experiments on light diffusion in anisotropic random media. Phys. Rev., E 62, 6681–6687.

Wölfle, P., Bhatt, R.N., 1984. Electron localization in anisotropic systems. Phys. Rev., B 30, 3542–3544.

Wu, R.S., 1982. Attenuation of short period seismic waves due to scattering. Geophys. Res. Lett. 9, 9–12.

Wu, R.S., 1985. Multiple scattering and energy transfer of seismic waves–separation of scattering effect from intrinsic attenuation: I. Theoretical modeling. Geophys. J. R. Astron. Soc. 82, 57–80.

Zeng, Y., 1993. Theory of scattered P- and S-wave energy in a random isotropic scattering medium. Bull. Seismol. Soc. Am. 83, 1264–1276.

Zeng, Y., Su, F., Aki, K., 1991. Scattering wave energy propagation in a random isotropic scattering medium 1. Theory. J. Geophys. Res. 96, 607–619.

Zhu, J.X., Pine, D.J., Weitz, D.A., 1991. Internal reflection of diffusive light in random media. Phys. Rev., A 44, 3948–3959.